





ORIGINAL ARTICLE

Impact of uncertainties in biometric parameters on intraocular lens power formula predicted refraction using a Monte-Carlo simulation

Achim Langenbucher¹  | Peter Hoffmann² | Alan Cayless³ | Matthias Bolz⁴  |
 Jascha Wendelstein^{1,4}  | Nóra Szentmáry^{5,6} 

¹Department of Experimental Ophthalmology, Saarland University, Homburg, Germany

²Augen- und Laserklinik Castrop-Rauxel, Castrop-Rauxel, Germany

³School of Physical Sciences, The Open University, Milton Keynes, UK

⁴Department of Ophthalmology, Johannes Kepler University Linz, Austria

⁵Dr. Rolf M. Schwiete Center for Limbal Stem Cell and Aniridia Research, Saarland University, Homburg, Germany

⁶Department of Ophthalmology, Semmelweis-University, Budapest, Hungary

Correspondence

Achim Langenbucher, Department of Experimental Ophthalmology, Saarland University, Kirrberger Str 100 Bldg. 22, 66424 Homburg, Germany.
 Email: achim.langenbucher@uks.eu

Abstract

Purpose: The purpose of this study was to investigate the uncertainty in the formula predicted refractive outcome REFU after cataract surgery resulting from measurement uncertainties in modern optical biometers using literature data for within-subject standard deviation S_w .

Methods: This Monte-Carlo simulation study used a large dataset containing 16667 preoperative IOLMaster 700 biometric measurements. Based on literature S_w values, REFU was derived for both the Haigis and Castrop formulae using error propagation strategies. Using the Hoya Vivinex lens (IOL) as an example, REFU was calculated both with (WLT) and without (WoLT) consideration of IOL power labelling tolerances.

Results: WoLT the median REFU was 0.10/0.12 dpt for the Haigis/Castrop formula, and WLT it was 0.13/0.15 dpt. WoLT REFU increased systematically for short eyes (or high power IOLs), and WLT this effect was even more pronounced because of increased labelling tolerances. WoLT the uncertainty in the measurement of the corneal front surface radius showed the largest contribution to REFU, especially in long eyes (and low power IOLs). WLT the IOL power uncertainty dominated in short eyes (or high power IOLs) and the uncertainty of the corneal front surface in long eyes (or low power IOLs).

Conclusions: Compared with published data on the formula prediction error of refractive outcome after cataract surgery, the uncertainty of biometric measures seems to contribute with $\frac{1}{3}$ to $\frac{1}{2}$ to the entire standard deviation. REFU systematically increases with IOL power and decreases with axial length.

KEY WORDS

biometric measures, error propagation, IOL formula predicted refractive outcome, ISO labelling tolerances, Monte-Carlo simulation, within-subject standard deviation

1 | INTRODUCTION

Replacement of classical ultrasound technology with modern optical biometry has been a quantum leap in biometry prior to cataract surgery. Today, optical biometry is accepted as the gold standard, with ultrasound biometry restricted to clinical cases where optical measurements fail in very dense optical media (Scholtz et al., 2021; Langenbucher et al., 2022). Without reference measurements, the accuracy of ultrasound or optical biometric measures cannot be validated directly (Hirnschall et al., 2020; Norrby et al., 1996; Preußner et al., 2008; Wendelstein et al., 2022), but the repeatability of the

results with optical techniques is far higher compared to ultrasound (Preußner et al., 2008; Haigis et al., 2000). In addition, optical biometry can easily be delegated to assistance staff since local anaesthesia is not required and the measurement is performed without contact. Also, with sufficient patient fixation the measurement is performed strictly along the fixation axis (Scholtz et al., 2021). Optical biometry provides direct data on all distances in the eye, including: axial length (AL in mm), central corneal thickness (CCT in mm), aqueous depth measured from the corneal endothelium to the lens front apex (AQD in mm), the (external) anterior chamber depth (ACD in mm, defined as the distance from the corneal epithelium

This is an open access article under the terms of the [Creative Commons Attribution-NonCommercial-NoDerivs](https://creativecommons.org/licenses/by-nc-nd/4.0/) License, which permits use and distribution in any medium, provided the original work is properly cited, the use is non-commercial and no modifications or adaptations are made.

© 2023 The Authors. *Acta Ophthalmologica* published by John Wiley & Sons Ltd on behalf of Acta Ophthalmologica Scandinavica Foundation.

to the lens front apex), and the central thickness of the crystalline lens (LT in mm), together with keratometric measures on the corneal front surface curvature (radii R_{1a} and R_{2a} in the flat and steep corneal meridians both in mm, mean radius R_a in mm) and optionally the radius data from the corneal back surface curvature (R_p in mm) (Fişuş et al., 2021). In addition, biometers yield data on horizontal corneal diameter, pupil diameter, and also on chord mu, the vector between the X/Y coordinates of the Purkinje I image and the pupil centre, which gives some information on the angle between the 'symmetry axis' of the eye and the 'visual axis'. Many modern intraocular lens (IOL) power calculation formulae have been adapted to the supplementary data provided by optical biometers and consider additional data such as ACD, LT, and the corneal diameter in addition to the basic data AL and keratometry ($K=(n_K-1)/R_a$ in dpt; a measure for corneal refractive power derived from the front surface radius R_a using a keratometer index n_K) in order to derive the appropriate IOL power (IOLP) (Scholtz et al., 2021).

However, we should be aware that all biometric measures show some amount of uncertainty. Within the last decade, many scientific studies have been performed focusing on the precision and repeatability of the measures of modern optical biometers, describing statistical metrics such as within-subject standard deviations S_w , coefficient of variation (CoV), or intra-class correlation coefficients (ICC) (Fişuş et al., 2021; Bullimore et al., 2019; Cheng et al., 2022; Ferrer-Blasco et al., 2017; Galzignato et al., 2023; Garza-Leon et al., 2017; Huang et al., 2017; Kunert et al., 2016; Martínez-Albert et al., 2019; Savini et al., 2021; Schiano-Lomoriello et al., 2021; Shetty et al., 2021; Wylęgała et al., 2020). From a sequence of at least three repeat measurements performed after re-adjustment of the patient's head and the biometer, such variation metrics give information on the consistency of the parameters in terms of repeatability (precision), but we have to keep in mind that the 'true values' (in terms of absolute accuracy) are still unknown (Hirnschall et al., 2020; Norrby et al., 1996; Preußner et al., 2008). Such uncertainties in the biometric measures (Norrby, 2008) have a direct impact on the formula predicted lens power. In other words, variation in the biometric measures will produce variation in the IOLP derived from these predictors. For any given lens model with a specific IOLP the resulting formula predicted refraction at the spectacle plane (REF) will show some uncertainty (Langenbacher et al., 2022; Lumme et al., 2015; Norrby, 2008; Norrby et al., 1996). The impact of uncertainties in the biometric measures on the target parameter (either IOLP or REF) is typically derived using a classical Gaussian error propagation (Lumme et al., 2015), which is restricted to a normal distribution of the uncertainty in all relevant predictors (described by the within-subject standard deviation S_w). The uncertainty of the target parameter (IOLP or REF) is again simplified to a normal distribution (Preußner et al., 2008; Lumme et al., 2015). Calculation of the error propagation requires either algebraic or numerical derivatives of the IOLP or REF formula with respect to the predictors (Lumme et al., 2015). Where interactions between the error metrics are known, those correlations can be considered using the covariance

matrix. Alternatively, fully data-driven calculation strategies could be used, based on a Monte-Carlo simulation model, where for each scenario many thousands of predictor combinations within the limits of the S_w distributions are tested to extract the distribution of the uncertainty in the target parameter (Lumme et al., 2015; Norrby, 2008; Norrby et al., 1996).

In most setups error propagation is restricted to a calculation based on the mean values of the predictors, taken together with the respective uncertainties S_w to derive the uncertainty of the target parameter (Lumme et al., 2015; Preußner et al., 2008). However, and especially with highly nonlinear formulae which transfer the predictors to the target parameter, such a simplification may fail as the resulting uncertainty of the target parameter depends strongly on the combination of all the predictor values. In our special case this means that, e.g. for large or small values of AL or R_a the resulting uncertainty in IOLP or REF may differ systematically.

The purpose of this paper is to investigate the impact of uncertainties in preoperative biometric measures on the uncertainty of the formula predicted refraction at the spectacle plane, based on a large clinical dataset containing measurements of a cataractous population taken prior to cataract surgery using a modern optical biometer, and to analyse this impact of the biometric uncertainties as a function of the formula predicted intraocular lens power IOLP, the axial length AL, and the corneal front surface radius R_a , by means of a Monte-Carlo simulation.

2 | METHODS

2.1 | Dataset for the prediction model

A large dataset containing 21 108 biometric measurements was considered in this study. All measurements were performed at Augen- und Laserklinik, Castrop-Rauxel, Germany and Department of Ophthalmology and Optometry, Johannes-Kepler-University Linz, Austria with the IOLMaster 700 (Carl-Zeiss Meditec).

After excluding eyes with any history of ocular surgery or documented comorbidities in the patient record, the data were anonymised at source and transferred to a .csv data table using the software module for batch data export. Data tables were reduced to the relevant parameters required for our data analysis and finally contained the following measurements: from the measurement before cataract surgery we extracted the patient's age (Age) in years, the laterality (left or right eye), sex (female or male), flat (R_{1a}) and steep (R_{2a}) corneal front surface radii of curvature both in mm, axial length (AL) in mm, central corneal thickness (CCT) in mm, anterior chamber depth (ACD) in mm (measured from corneal epithelium to lens), central thickness of the crystalline lens (LT) in mm, and horizontal corneal diameter (CD) in mm. Data with AL/ACD/ R_{1a} / R_{2a} measurements outside the interval 18–34 mm/1.8–4.3 mm/6.0–9.5 mm/6.0–9.5 mm were excluded from the dataset. Only one eye from each subject was included in this study. Where measurements of both eyes were available, one eye was randomly selected. Subjects with missing data or data other than 'OK' in the internal

quality check of the IOLMaster 700 for R_{1a} , R_{2a} , AL, CCT, ACD, LT and CD were excluded from the dataset.

The local Institutional Review Board provided a waiver for this retrospective study (Ethikkommission der Ärztekammer des Saarlandes, registration number 157/21), and informed consent from the patient was not required. The data were transferred to Matlab (2022b; MathWorks) for further processing.

2.2 | Data pre-processing in Matlab

The mean corneal front surface radius R_a in mm was calculated as $R_a = 0.5 (R_{1a} + R_{2a})$. For IOLP calculation we implemented the Haigis formula (Haigis et al., 2000) as an example of a fully disclosed 4th generation lens power calculation formula based on R_a , AL, and ACD, and also the Castrop formula (Wendelstein et al., 2022; Langenbucher, Szentmáry, Cayless, Weisensee, Fabian, et al., 2021; Langenbucher, Szentmáry, Cayless, Weisensee, Wendelstein, & Hoffmann, 2021) as a modern lens power calculation formula dealing with a thick lens model for the cornea and an effective lens position prediction which mimics the anatomically correct axial position of the IOL in the pseudophakic eye. To simplify the data interpretation, the corneal back surface radius was derived from a fixed proportion of front to back surface radii (7.77/6.4 mm) according to the Liou & Brennan schematic model eye (Liou & Brennan, 1997). For our calculations we considered a commonly used IOL model (Hoya Vivinex XC1, Hoya surgical) as a typical example. This lens model has a delivery range from 6.0 to 30.0 dpt and power steps of 0.5 dpt over the entire power range. The respective formula constants for the Haigis formula (Haigis et al., 2000) ($a_0/a_1/a_2 = -1.0643/0.2580/0.23010$) and the Castrop formula (Wendelstein et al., 2022; Langenbucher, Szentmáry, Cayless, Weisensee, Fabian, et al., 2021; Langenbucher, Szentmáry, Cayless, Weisensee, Wendelstein, & Hoffmann, 2021) ($C/H/R = 0.3249/0.1267/0.1548$) were extracted from the IOLCon WEB platform (<https://IOLCon.org>, accessed on 09/04/2023). Using both the Haigis and the Castrop formula the 'exact' lens power ($IOLP_H$ and $IOLP_C$ both in dpt) was calculated for a target refraction of $TR = -0.125$ dpt, chosen to avoid hyperopia after cataract surgery. The $IOLP_H$ and $IOLP_C$ were subsequently rounded to the closest available power step ($IOLP_{HS}$ and $IOLP_{CS}$ both in dpt). Cases with $IOLP_H$ or $IOLP_C$ less than 5.75 dpt or higher than 30.25 dpt were considered to be out of the delivery range of the Vivinex lens.

2.3 | Uncertainties of the biometric measures and IOL power

Based on a literature search the characteristic within-subject standard deviations were evaluated and taken as uncertainties for the biometric measures (Fişuş et al., 2021; Bullimore et al., 2019; Cheng et al., 2022; Ferrer-Blasco et al., 2017; Galzignato et al., 2023; Garza-Leon et al., 2017; Huang et al., 2017; Kunert et al., 2016;

Martínez-Albert et al., 2019; Savini et al., 2021; Schiano-Lomoriello et al., 2021; Shetty et al., 2021; Wylęgała et al., 2020). From these literature data we extracted the following S_w values to be used in our error propagation calculations (Savini et al., 2021; Shetty et al., 2021): AL: $S_wAL = 0.022$ mm, CCT: $S_wCCT = 5.626$ μ m, ACD: $S_wACD = 0.017$ mm, LT: $S_wLT = 0.041$ mm, K : $S_wK = 0.08$ dpt. As no direct S_w data were available in the literature for the corneal front surface radius R_a , we converted all R_a values in our dataset to K values using $n_K = 1.3375$ (Savini et al., 2021 as specified in the literature with the within-subject standard deviation data) and calculated the uncertainty in R_a with a variation of $\pm S_wK$ as $\Delta R_a = 337.5 (1/[K - S_wK] - 1/[K + S_wK])$. The within-subject standard deviation for R_a was then estimated as $S_wR_a = 0.5 \Delta R_a$ (Lumme et al., 2015).

For the IOLP we also optionally considered a labelling tolerance. ISO 11979 specifies the IOLP labelling tolerances as a function of IOLP (2014 Ophthalmic Implants – Intraocular lenses: EN ISO 11979-2). Labelling tolerances were assumed to be normally distributed with a standard deviation of $S_wIOL = 1/3$ of the tolerances, according to the ISO standard as proposed by Norrby. This value is chosen to ensure that (based on a normal distribution) at least 99% of the lens power data are within the ISO tolerances (Norrby, 2008). For lens power values $IOLP_{HS}/IOLP_S$ from 6.0 to 15 dpt we assumed $S_wIOL = 0.1$ dpt, for lens powers from 15.5 to 25.0 dpt we assumed $S_wIOL = 0.1333$ dpt, and for lens powers of 25.5–30.0 dpt we assumed $S_wIOL = 0.1667$ dpt (Norrby, 2008).

2.4 | Error propagation and Monte–Carlo simulation

As a first step we evaluated the differences between different error propagation strategies. For the Haigis formula the parameters R_a , AL and ACD were used as predictors and for the Castrop formula R_a , AL, CCT, ACD and LT were used as predictors. In our simulation we assumed that the measurement uncertainties in the predictors are uncorrelated (Lumme et al., 2015) (as there are no data available in the literature on interactions between errors in repeat measurements). We implemented an error propagation calculation based on (A) the algebraic calculation of the gradient of the REF prediction formula, (B) the numerical calculation of the gradient of the REF prediction formula, and (C) a fully data-driven Monte–Carlo simulation (1 000 000 sweeps) based on normally distributed variations of the predictors. Figure 1 shows the distributions of the formula predicted REF uncertainty (REFU) for (A) (upper graphs), (B) (middle graphs), and (C) (lower graphs) for the Haigis formula (left column of graphs) and the Castrop formula (right column of graphs), all for the first data point in the dataset as an example. Since we did not find any systematic difference between (A), (B), and (C) for either the Haigis (Haigis et al., 2000) or the Castrop formula (Wendelstein et al., 2022; Langenbucher, Szentmáry, Cayless, Weisensee, Fabian, et al., 2021; Langenbucher, Szentmáry, Cayless, Weisensee, Wendelstein, & Hoffmann, 2021) we decided to consider the numerical calculation of the gradient of

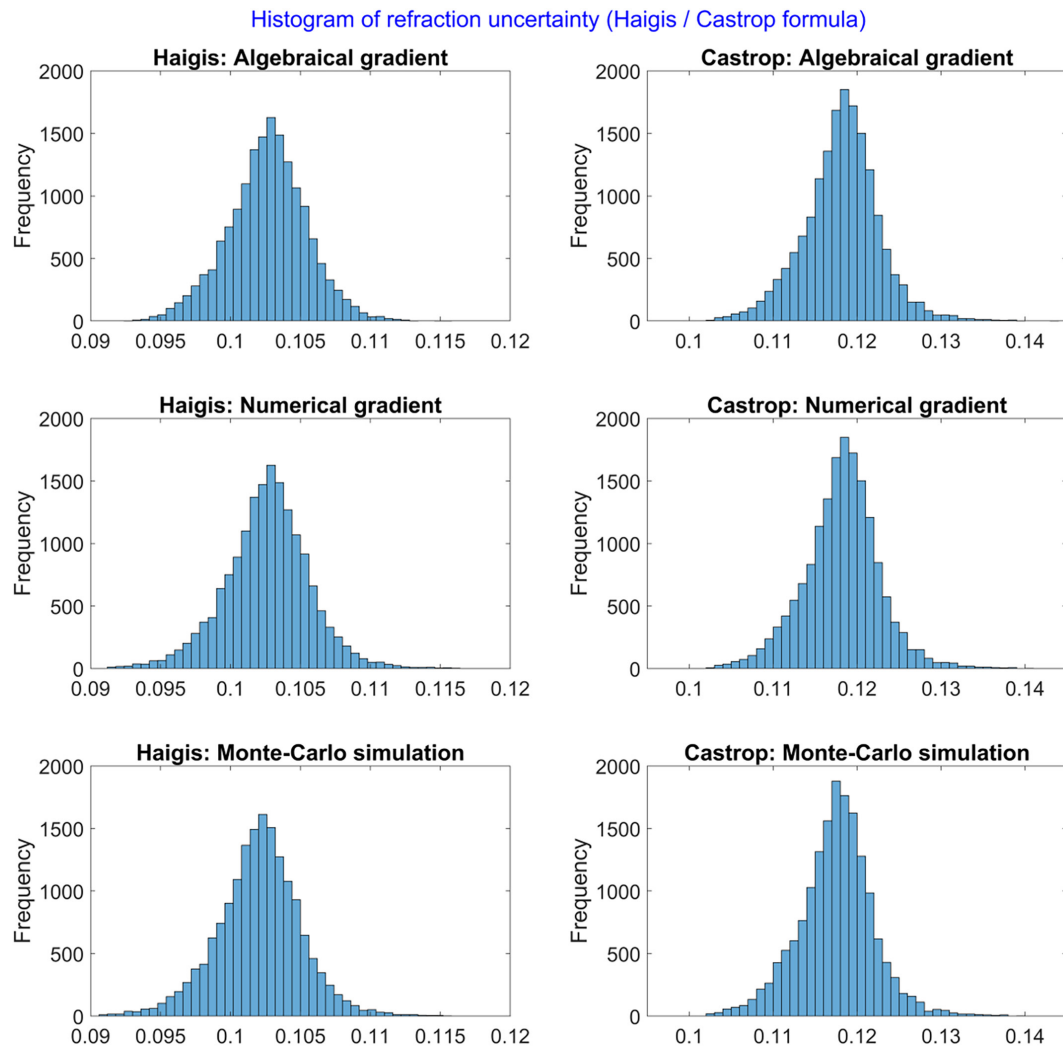


FIGURE 1 Histograms for the refraction uncertainty distribution at the spectacle plane, for the example of the first data point (case 1) in our dataset. The refraction uncertainty was calculated based on the uncertainties of the biometric predictors (axial length AL, anterior chamber depth ACD, corneal front surface radius R_a for the Haigis and AL, central corneal thickness CCT, ACD, crystalline lens thickness LT and R_a for the Castrop formula) using an error propagation model based on algebraic gradients (upper row), numerical gradients (middle row), or a Monte–Carlo simulation (lower row) with 1 000 000 sweeps. There is no relevant difference between the different settings for the Haigis or the Castrop formula; therefore we decided to perform further analysis based on numerical gradients.

the REF prediction formula (A) for our analysis (Lumme et al., 2015).

All error propagation calculations were performed for variation of all biometric predictors, both with and without consideration of uncertainties in IOLP power due to labelling tolerances.

In the last step we recalculated all error propagation simulations, leaving the variation of one parameter out in turn, in order to investigate the impact of each biometric measure (or the variation of the lens power according to ISO labelling tolerances) on REFU. This means that for the Haigis formula we nullified either $S_w R_a$, $S_w AL$, or $S_w ACD$ (without consideration of ISO tolerances) or $S_w R_a$, $S_w AL$, $S_w ACD$, or $S_w IOL$ (with consideration of ISO tolerances). For the Castrop formula we nullified either $S_w R_a$, $S_w AL$, $S_w CCT$, $S_w ACD$ or $S_w LT$ (without consideration of ISO tolerances), or $S_w R_a$, $S_w AL$, $S_w CCT$; $S_w ACD$, $S_w LT$ or $S_w IOL$ (with consideration of ISO tolerances).

2.5 | Statistical evaluation

Explorative data analysis in tables was performed for the arithmetic mean, the SD, the median, and the lower and upper boundary of the 95% confidence interval (which refers to the 2.5% and 97.5% quantiles).

According to Lumme et al. the 68% confidence intervals (CI) were identified in the uncertainty distribution of the formula predicted REF by individually searching for the shortest interval in the data containing 68% of the entire refraction data at the spectacle plane (Lumme et al., 2015). Half of this confidence interval (0.5·CI) was considered as the uncertainty measure for the refraction REFU due to uncertainties in the biometric parameters or the IOLP labelling tolerance. REFU was evaluated as a function of the formula predicted IOLP (IOLP_H or IOLP_C), the axial length AL, and the corneal front surface radius R_a .

3 | RESULTS

From the $N=21\,108$ data points transferred to us, and after considering the selection criteria, a dataset with $N=16\,667$ eyes of 16 667 patients was considered for our analysis ($N=9\,284$ eyes from the Augen- und Laserklinik Castrop-Rauxel, $N=7\,383$ eyes from the Department of Ophthalmology, Johannes-Kepler-University Linz). In total, 8405 left and 8262 right eyes from 7107 male and 9560 female patients were included. Table 1 lists the descriptive data for the ocular biometry before cataract surgery including age, AL, CCT, ACD, LT, CD, and R_a together with the formula predicted power IOLP_H and IOLP_C for a target refraction of -0.125 dpt.

According to the Haigis/Castrop formula an adequate lens within the delivery range of the Vivinex IOL could be calculated for $N=16\,380$ (98.28%)/ $N=16\,406$ (98.43%) of the eyes in the dataset respectively.

Figure 2 displays the refraction uncertainty at the spectacle plane REFU resulting from uncertainty in the biometric measures without considering the labelling tolerances for the IOLP for the Haigis formula (upper graph) and for the Castrop formula (lower graph). The total uncertainty REFU values are plotted as brown dots (red scale on the Y axis right side) along with the contribution of each biometric measure (AL, CCT, ACD, LT, R_a for the Castrop and AL, ACD, R_a for the Haigis formula) to REFU in % (blue scale on the Y axis left side). REFU is plotted as a function of the formula predicted lens power (IOLP_H or IOLP_C, upper graph), the axial length AL (middle graph), and the corneal front surface radius R_a (lower graph). We can see directly from the upper two graphs for both formulae that in both cases REFU increases systematically for short eyes (small AL values) requiring high power IOLs (large values of IOLP_H and IOLP_C) whereas the lower of the three graphs in each case shows that the corneal front surface radius has only a very small effect on REFU (REFU increases slightly for steeper corneas with small values of R_a with either formula). The uncertainty in R_a dominates REFU over the entire range of AL or lens power. In long eyes especially, R_a contributes up to 70% to REFU, but even in short eyes R_a contributes around 30%. The uncertainty in AL contributes around 5%–8% to REFU in long eyes and 20%–25% in short eyes, whereas the uncertainty in ACD or the uncertainty in CCT and LT (for the Castrop

formula) seem to have no clinically relevant impact on REFU.

Figure 3 displays the refraction uncertainty at the spectacle plane REFU resulting from uncertainty in the biometric measures and also considering the labelling tolerances for the IOLP for the Haigis formula (upper graph) and for the Castrop formula (lower graph). The total uncertainty REFU values are plotted as brown dots (red scale on the Y axis right side) along with the contribution of each biometric measure and the IOL labelling tolerance (AL, CCT, ACD, LT, R_a and IOL for the Castrop; AL, ACD, R_a and IOL for the Haigis formula) to REFU in % (blue scale on the Y axis left side). REFU is plotted as a function of the formula predicted lens power (IOLP_H or IOLP_C, upper graph), the axial length AL (middle graph), and the corneal front surface radius R_a (lower graph). We can see directly from the upper two graphs in each case that for both the Haigis and the Castrop formula REFU systematically increases for short eyes (small AL values) requiring high power IOLs (large values of IOLP_H and IOLP_C). According to the ISO labelling tolerances REFU shows some step formation at IOLP_H/IOLP_C equal 15 and 25 dpt (upper graphs) and this is also reflected in a mild form in the middle graphs with REFU as a function of AL. Again, the lower of the three graphs in each case shows that the corneal front surface radius has only a very small effect on REFU (REFU increases slightly for steeper corneas with small values of R_a). The uncertainty in R_a dominates REFU in long eyes (around 35%–40% with large AL values), whereas the IOL labelling tolerance contributes the most to REFU for short eyes (around 30% to 35% with small AL values). The uncertainty in AL contributes around 5%–12% to REFU (especially in short eyes), whereas the uncertainty in ACD or the uncertainty in CCT and LT (for the Castrop formula) seems to have no clinically relevant impact on REFU (in a range below 3%).

Table 2 displays the explorative data of the predicted refraction uncertainty at the spectacle plane REFU based on the Haigis and the Castrop formula for the 16 406/16 380 cases in the dataset ($N=16\,667$) where the formula predicted lens power was within the delivery range of the Vivinex IOL. For the option ‘without IOL labelling error’ for the Haigis formula/Castrop formula the uncertainties in the biometric parameters axial length AL, anterior chamber depth ACD and corneal

TABLE 1 Explorative data of patient age at the time point of measurement, axial length (AL), central corneal thickness (CCT), anterior chamber depth (ACD) measured from corneal epithelium to lens front apex, thickness of the crystalline lens (LT), horizontal corneal diameter (CD), mean corneal front surface radius (R_a), and the Haigis/Castrop formula predicted lens power (IOLP_H/IOLP_C) for a target refraction of TR = -0.125 dpt.

$N=16\,667$	Age in years	AL in mm	CCT in mm	ACD in mm	LT in mm	CD in mm	R_a in mm	IOLP _H in dpt	IOLP _C in dpt
Mean	70.5	23.7886	0.5515	3.2253	4.4514	11.9906	7.7161	20.489	20.456
Standard deviation	9.5	1.4083	0.0367	0.3768	0.3956	0.4106	0.2725	4.169	4.169
Median	72.0	23.5886	0.5509	3.2154	4.5249	11.9873	7.7100	21.127	21.127
2.5% quantile	49.0	21.5962	0.4818	2.5058	3.3857	11.1955	7.2050	10.204	10.204
97.5% quantile	86.0	27.1742	0.6250	3.9791	4.9697	12.7985	8.2750	27.331	27.332

Note: The table lists the arithmetic mean, standard deviation, median, and the lower and upper boundary of the 95% confidence interval (2.5% and 97.5% quantiles).

front surface radius R_a /axial length AL, central corneal thickness CCT, anterior chamber depth ACD, crystalline lens thickness LT, and corneal front surface radius R_a were considered. For the option ‘with IOL labelling tolerances’ the tolerances in the intraocular lens power labels were considered in addition to these biometric parameters.

4 | DISCUSSION

The improvements in ocular biometry and intraocular lens power calculation can be seen as the preconditions for new features in modern intraocular lenses such as monofocal plus, enhanced depth of focus EDOF, multifocal, accommodating, and toric lenses. The requirements for a conscientious use of these new technologies (e.g. in terms of reaching the target refraction) can only be fulfilled with optical biometry in combination with modern advanced IOLP calculation strategies. However,

optical biometry does not solve all problems in cataract surgery: first, the true biometric values in a patient's eye are unknown and cannot be directly measured; second, all biometric values show some variation with repeat measurements, and the uncertainties in the biometric measures have to be propagated to an uncertainty in the target parameters, namely the formula predicted lens power or refraction; third, we have to predict the condition of the pseudophakic eye before cataract surgery, and parameters may somehow change due to surgery (e.g. corneal power or astigmatism) or the measurement conditions (e.g. due to unknown refractive index of ocular media); fourth, all calculation strategies work with simplifications and assumptions, and the validity of these simplifications cannot be verified during lens power calculation; fifth, the labelled lens power on the package may deviate from the true lens power or may not fully reflect the optical properties of the ‘thick lens’ IOL. Many optical biometers have been launched to the market in the last decade, and all have been extensively tested

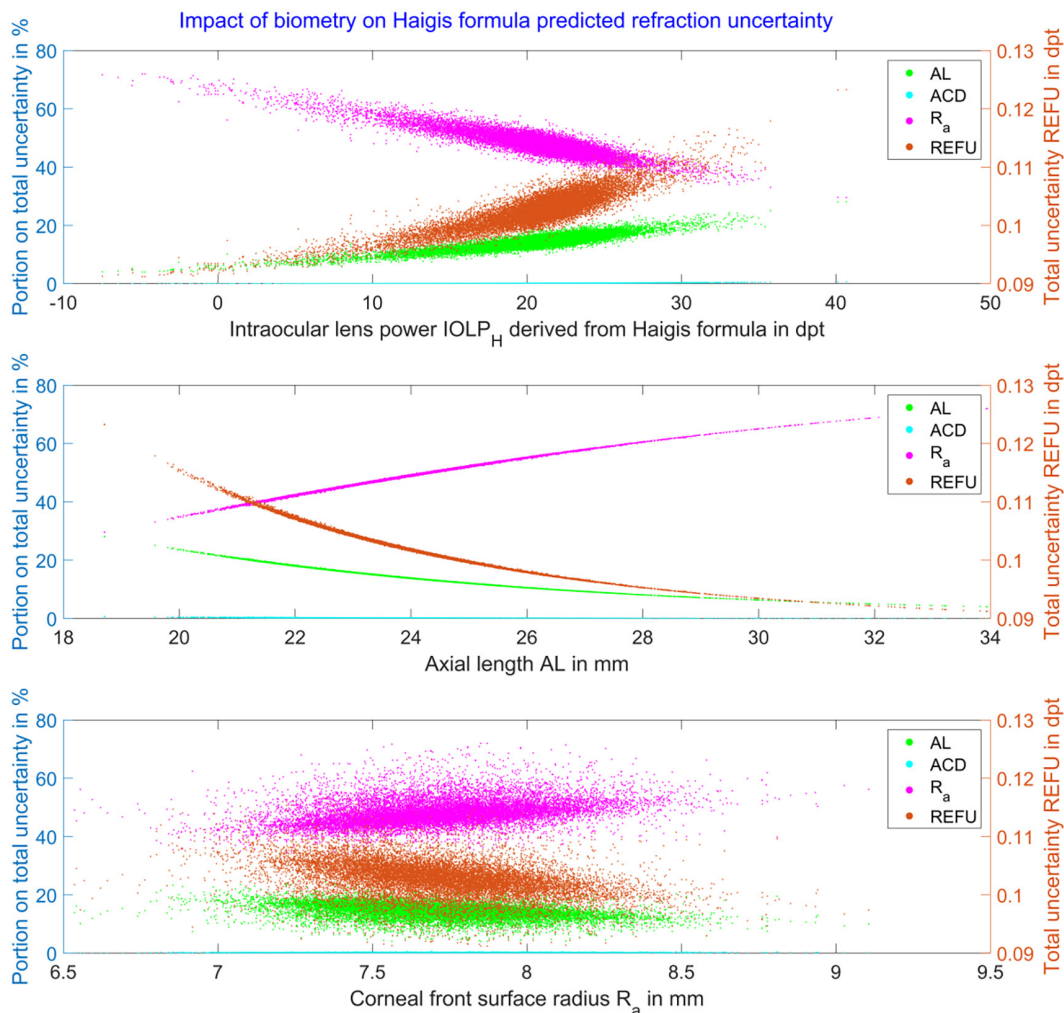


FIGURE 2 Refraction uncertainty at the spectacle plane REFU resulting from uncertainty in the biometric measures without considering the labelling tolerances for the IOLP for the Haigis formula (upper three graphs) and the Castrop formula (lower three graphs). The total uncertainty REFU values are plotted as brown dots (red scale on the Y axis right side) along with the contribution of each biometric measure (AL, CCT, ACD, LT, R_a for the Castrop and AL, ACD, R_a for the Haigis formula) on REFU in % (blue scale on the Y axis left side). Please note that the uncertainties do not superimpose linearly, with the consequence that the contributions do not add to 100%. In each case, REFU is plotted as a function of the formula predicted lens power ($IOLP_H$ or $IOLP_C$, upper graph), the axial length AL (middle graph), and the corneal front surface radius R_a (lower graph). We directly see from the graphs that for both formulae REFU systematically increases for short eyes requiring high power IOLs. The uncertainty in R_a dominates REFU over the entire range of AL or lens power (especially in long eyes). The uncertainty in AL contributes around 5%–8% to REFU in long eyes and 20%–25% in short eyes.

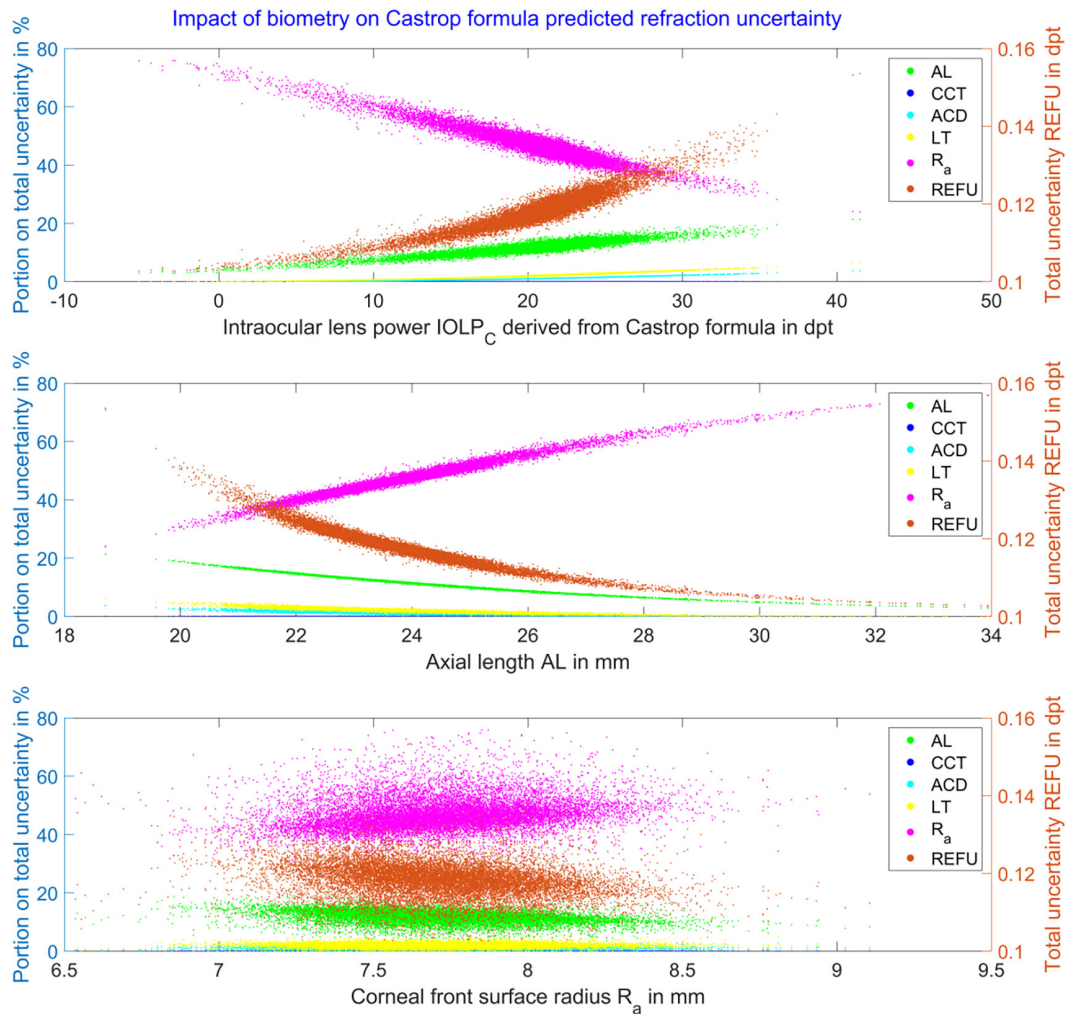


FIGURE 2 (Continued)

for repeatability or reproducibility (Fişuş et al., 2021; Bullimore et al., 2019; Cheng et al., 2022; Ferrer-Blasco et al., 2017; Galzignato et al., 2023; Garza-Leon et al., 2017; Huang et al., 2017; Kunert et al., 2016; Martínez-Albert et al., 2019; Savini et al., 2021; Schiano-Lomoriello et al., 2021; Shetty et al., 2021; Wylęgała et al., 2020) and compared against others to evaluate the coherence of the biometric measures (Asawaworarit et al., 2022; Asena et al., 2018; Huang et al., 2019; Lu et al., 2019; Panthier et al., 2022; Sabatino et al., 2016; Sabatino et al., 2019). Typically a sequence of 3–5 measurements is performed in a set of patients and characteristic metrics such as the within-subject standard deviations S_w extracted. Such metrics mostly rely on a normal distribution of the data scatter with repeat measurements. Much larger sequences of repeat measurements have to be performed in order to estimate the distribution of the error. All of these data are restricted in precision, and the absolute accuracy cannot be evaluated as the true values for the biometric measures are unknown. In addition, we have not found any studies that focus on the correlations between the uncertainties of repeat biometric measures. For example, for the Zeiss IOLMaster 700, we find S_w values in a range of 0.069–0.32 dpt for K , 2–8 μm for CCT, up to 0.23 mm for CD, up to 0.05 mm for ACD, 0.01–0.07 mm for LT, and up to 0.025 mm for AL (Fişuş et al., 2021; Bullimore et al., 2019; Cheng et al., 2022;

Ferrer-Blasco et al., 2017; Galzignato et al., 2023; Garza-Leon et al., 2017; Huang et al., 2017; Kunert et al., 2016; Martínez-Albert et al., 2019; Savini et al., 2021; Schiano-Lomoriello et al., 2021; Shetty et al., 2021; Wylęgała et al., 2020). Especially for K the literature data are very inconsistent with a large range of variation. For our error propagation model we eventually decided to use the S_w data for AL, CCT, ACD and LT shown by Shetty et al., since these were based on the largest patient cohort with $N=127$ cases (Shetty et al., 2021). For the S_w values of keratometry we used the data of Savini et al. as this study focused on repeatability of keratometry and total keratometry and the S_w for the mean corneal front surface radius R_a was explicitly mentioned (Savini et al., 2021).

Different error propagation techniques are available. When dealing with normally distributed uncertainties of the predictors, classical concepts which use the gradient of the linear or nonlinear transfer function to convert the predictor variables to an uncertainty of the target parameter are appropriate (Lumme et al., 2015). Therefore, we implemented three different strategies including the algebraic gradient, the numerical gradient, and a more general Monte–Carlo-based method which is not restricted to a normal distribution of the uncertainty of the predictors and can be used with any uncertainty distribution (Lumme et al., 2015). What we found is that the distribution of the uncertainty in refraction at the

spectacle plane shows no clinically relevant differences between the three strategies (as shown in Figure 1). We therefore decided to concentrate on the numerical gradient of the transfer function with respect to the biometric predictors to calculate REFU. This was defined as half the width of the 68% confidence interval of the uncertainty distribution of refraction at the spectacle plane (Lumme et al., 2015). Where distributions of measurement uncertainties other than normal distributions are to be considered we have to switch to a Monte–Carlo simulation.

After calculation using the Haigis (Haigis et al., 2000) and Castrop formula (Wendelstein et al., 2022; Langenbucher, Szentmáry, Cayless, Weisensee, Fabian, et al., 2021; Langenbucher, Szentmáry, Cayless, Weisensee, Wendelstein, & Hoffmann, 2021) of the ‘exact’ lens power to achieve a target refraction of $TR = -0.125$ dpt to avoid hyperopia after cataract surgery, we rounded this lens power to the closest available

power step. The Hoya Vivinex lens was used as an example of a current modern IOL design. This lens model is available in a power range from 6 to 30 dpt in steps of half dioptres. Eyes requiring lenses outside this delivery range were excluded from the analysis. For all remaining eyes we propagated (A) the uncertainties in the biometric parameters and (B) the uncertainties in both the biometric parameters and the labelling tolerances to REFU in order to obtain an idea of the amount of intrinsic background noise in intraocular lens power calculation which cannot be overcome even with very advanced calculation strategies. Given a lack of measurement data on the real labelling error of the IOLs, we used the data of Norrby who estimated the standard deviation of the labelling error as 1/6 of the entire range according to the ISO 11979 standard (Norrby, 2008) (1/3 of the tolerance). From Table 2 we learn that the median REFU based on the biometric parameter uncertainties from the literature is 0.1027/0.1188 dpt for the Haigis/Castrop

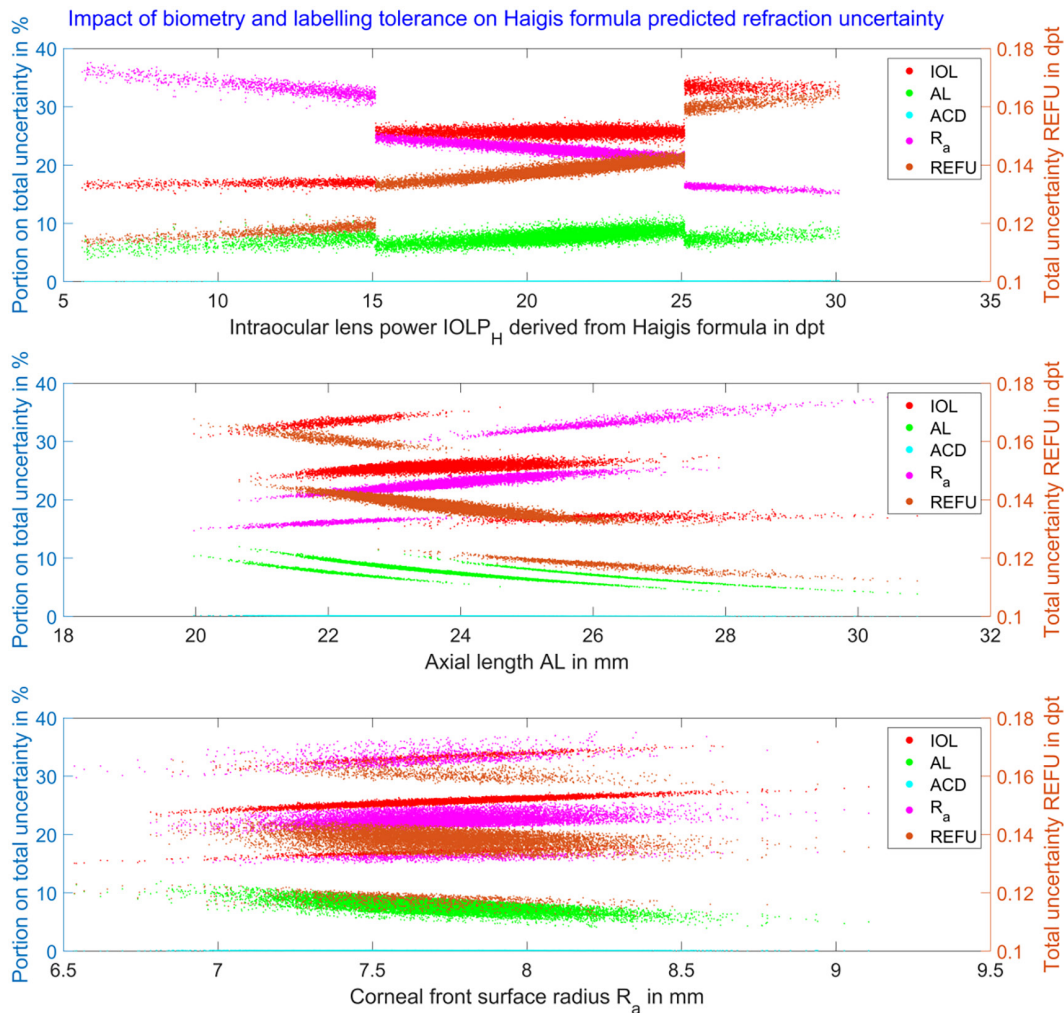


FIGURE 3 Refraction uncertainty at the spectacle plane REFU resulting from uncertainty in the biometric measures and also considering the labelling tolerances for the IOLP for the Haigis formula (upper three graphs) and the Castrop formula (lower three graphs). The total uncertainty REFU values are plotted as brown dots (red scale on the Y axis right side) along with the contribution of each biometric measure and the IOL labelling tolerance (AL, CCT, ACD, LT, R_a and IOL for the Castrop; AL, ACD, R_a and IOL for the Haigis formula) on REFU in % (blue scale on the Y axis left side). Please note that the uncertainties do not superimpose linearly with the consequence that the contributions do not add to 100%. In each case, REFU is plotted as a function of the formula predicted lens power (IOLP_H or IOLP_C, upper graph), the axial length AL (middle graph), and the corneal front surface radius R_a (lower graph). We directly see from the graphs that for both formulae REFU systematically increases for short eyes requiring high power IOLs. According to the ISO labelling tolerances, REFU shows some step formation at IOLP_H/IOLP_C equal 15 and 25 dpt (upper graphs). The uncertainty in R_a dominates REFU in long eyes, whereas the IOL labelling tolerance contributes the most to REFU for short eyes. The uncertainty in AL contributes around 5%–12% to REFU, whereas the uncertainty in ACD or the uncertainty in CCT and LT (only Castrop formula) seems to have no clinically relevant impact on REFU.

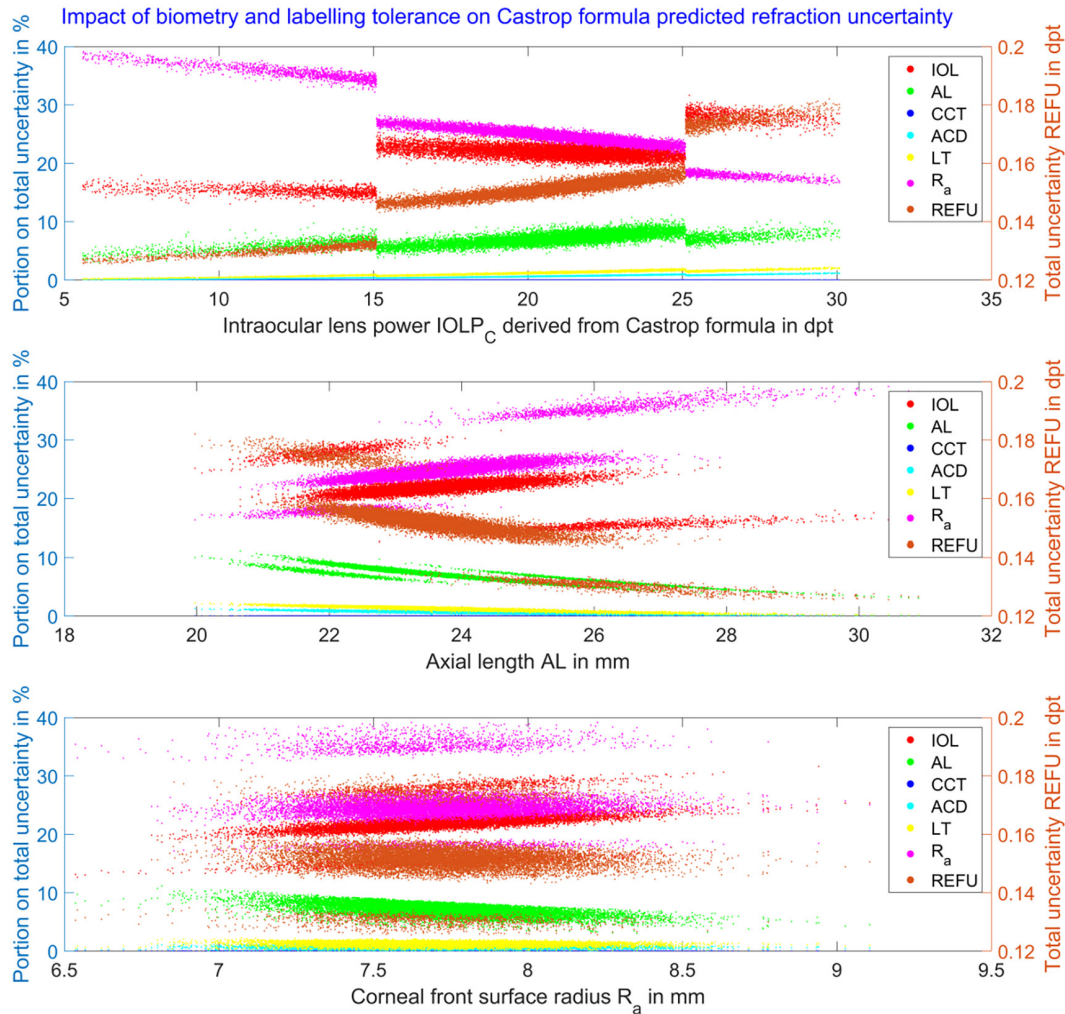


FIGURE 3 (Continued)

TABLE 2 Explorative data of the predicted refraction uncertainty at the spectacle plane REFU based on the Haigis and the Castrop formula.

REFU in dpt	Haigis formula (N=16380)		Castrop formula (N=16406)	
	Without IOL labelling tolerances	With IOL labelling tolerances	Without IOL labelling tolerances	With IOL labelling tolerances
Mean	0.1026	0.1380	0.1182	0.1512
Standard deviation	0.0030	0.0089	0.0045	0.0092
Median	0.1027	0.1383	0.1183	0.1516
2.5% quantile	0.0963	0.1167	0.1088	0.1294
97.5% quantile	0.1086	0.1612	0.1273	0.1749

For the option ‘without IOL labelling error’ for the Haigis formula/Castrop formula the uncertainty of the biometric parameters axial length (AL), anterior chamber depth (ACD) and corneal front surface radius (R_a)/axial length (AL), central corneal thickness (CCT), ACD, crystalline lens thickness (LT), and corneal front surface radius R_a were considered, respectively. For the option ‘with IOL labelling tolerances’ the tolerances in the intraocular lens power labels were considered in addition to these biometric parameters. The table lists the mean, standard deviation, median, and the lower and upper boundary of the 95% confidence interval (2.5% and 97.5% quantiles).

formula respectively. When the labelling tolerance of the IOL power is also taken into account, the median REFU values increase to 0.1388/0.1516 dpt. If we compare these data with the standard deviation of the formula prediction error for the refractive outcome with values in a range between 0.3 and 0.4 dpt (Wendelstein et al., 2022; Langenbucher, Szentmáry, Cayless, Weisensee, Fabian, et al., 2021; Langenbucher, Szentmáry, Cayless, Weisensee, Wendelstein, & Hoffmann, 2021), we see that

$\frac{1}{3}$ – $\frac{1}{2}$ of the standard deviation is already explained by the uncertainty in the biometric measures.

From Figure 2 we see that REFU systematically decreases with the AL and as a consequence increases with $IOLP_H/IOLP_C$, but that it shows only a slight dependency on R_a (mostly due to the conversion of S_w for K as provided in the literature, which had to be converted to S_w in R_a to be considered in the Haigis and Castrop formula). This finding is in accordance with

clinical observations that—especially in short eyes—the prediction of the refractive outcome is less reliable as compared to normal or long eyes. Interestingly, the contribution of the uncertainty in R_a to REFU is much larger compared to the contribution of the AL or ACD (Haigis and Castrop formula) and even more compared to the uncertainty of CCT or LT (Castrop formula), which is clinically negligible. Especially in long eyes which typically require low power IOLs the uncertainty of R_a seems to dominate REFU. When we consider the uncertainties of the IOL power labels in addition to the uncertainties of the biometric measures as shown in Figure 3, we notice some steps in REFU at a lens power of 15 and 25 dpt where the tolerances of the labelled lens power according to ISO 11979 change. Because the labelling tolerances for high power IOLs are wider compared to those for low power lenses (2014 Ophthalmic Implants – Intraocular lenses: EN ISO 11979-2), the effect of REFU increase for shorter eyes or larger IOLP values is further emphasised. For high power lenses (and short eyes) the uncertainty of the labelled IOLP contributes the most to REFU, whereas for low power lenses (long eyes) the uncertainty in the R_a measurement dominates REFU. Again, the uncertainty in AL measurement has much less impact on REFU, and ACD (Haigis formula) or CCT, ACD and LT (Castrop formula) seem to be negligible compared to uncertainty in R or the labelling error in the IOLP.

However, our study has some limitations: Firstly, we had to extract one set of S_w values from a variety of literature data on the within-subject standard deviation of biometric measures to be used for our error propagation study. Secondly, as the data distributions of the measurement uncertainties are not reported in the literature (mostly due to short sequences of repeat measurements) we assumed normal distributions for all the biometric measures. If distribution data were available for the biometric measure uncertainties, this could be directly considered using a Monte–Carlo simulation of REFU instead of using the algebraic or numerical gradient. Thirdly, we did not find any data on the interaction or correlations between the uncertainties of the biometric measures. Therefore we assumed that all measurement uncertainties were uncorrelated (covariance matrix as a diagonal matrix). Finally, we restricted our simulation to two fully disclosed vergence formulae (one with a thin and one with a thick lens model for the cornea) and for the IOL delivery range, power steps, and formula constants we selected those of a typical modern aspherical hydrophobic IOL currently on the market. If the simulations were performed with other formulae or a different lens model, we might expect slightly different results, but no relevant changes in the main findings.

5 | CONCLUSION

Our data indicate that based on literature data for the within-subject standard deviation of biometric data from repeat measurements, the formula predicted uncertainty of refraction at the spectacle plane REFU increases systematically in short eyes (or high power intraocular

lenses), whereas the corneal front surface radius R_a shows only a very slight effect on REFU. R_a contributes the most to REFU, especially on long eyes (or low power intraocular lenses), whereas the uncertainties of the axial length AL show a limited contribution to REFU. If we consider the uncertainty of the IOL power label in addition to the uncertainties of biometry, the increase in REFU for high power lenses (or short eyes) is even more pronounced. For long eyes (or low power lenses) the uncertainty of R_a contributes the most to REFU whereas for short eyes (or high power IOL) the uncertainty in the IOL power label dominates REFU.

ACKNOWLEDGEMENTS

Open Access funding enabled and organized by Projekt DEAL.

ORCID

Achim Langenbacher  <https://orcid.org/0000-0001-9175-6177>

Matthias Bolz  <https://orcid.org/0000-0001-8691-5276>

Jascha Wendelstein  <https://orcid.org/0000-0003-4145-2559>

Nóra Szentmáry  <https://orcid.org/0000-0001-8019-1481>

REFERENCES

- Asawaworarit, R., Satitpitakul, V., Taweekitkul, P. & Pongpirul, K. (2022) Agreement of total corneal power between 2 swept-source optical coherence tomography and Scheimpflug tomography in normal and keratoconic patients. *PLoS One*, 17(5), e0268856. Available from: <https://doi.org/10.1371/journal.pone.0268856>
- Asena, L., Akman, A., Güngör, S.G. & Dursun Altınörs, D. (2018) Comparison of keratometry obtained by a swept source OCT-based biometer with a standard optical biometer and Scheimpflug imaging. *Current Eye Research*, 43(7), 882–888. Available from: <https://doi.org/10.1080/02713683.2018.1458881>
- Bullimore, M.A., Slade, S., Yoo, P. & Otani, T. (2019) An evaluation of the IOLMaster 700. *Eye & Contact Lens*, 45(2), 117–123. Available from: <https://doi.org/10.1097/ICL.0000000000000552>
- Cheng, S.M., Zhang, J.S., Shao, X., Wu, Z.T., Li, T.T., Wang, P. et al. (2022) Repeatability of a new swept-source optical coherence tomographer and agreement with other three optical biometers. *Græfe's Archive for Clinical and Experimental Ophthalmology*, 260(7), 2271–2281. Available from: <https://doi.org/10.1007/s00417-022-05579-9>
- Ferrer-Blasco, T., Domínguez-Vicent, A., Esteve-Taboada, J.J., Aloy, M.A., Adsuara, J.E. & Montés-Micó, R. (2017) Evaluation of the repeatability of a swept-source ocular biometer for measuring ocular biometric parameters. *Græfe's Archive for Clinical and Experimental Ophthalmology*, 255(2), 343–349. Available from: <https://doi.org/10.1007/s00417-016-3555-z>
- Fişuş, A.D., Hirnschall, N.D., Ruiss, M., Pilwachs, C., Georgiev, S. & Findl, O. (2021) Repeatability of 2 swept-source OCT biometers and 1 optical low-coherence reflectometry biometer. *Journal of Cataract & Refractive Surgery*, 47(10), 1302–1307. Available from: <https://doi.org/10.1097/j.jcrs.0000000000000633>. Erratum in: (2022): *Journal of Cataract and Refractive Surgery* 48(6):750.
- Galzignato, A., Lupardi, E., Hoffer, K.J., Barboni, P., Schiano-Lomoriello, D. & Savini, G. (2023) Repeatability of new optical biometer and agreement with 2 validated optical biometers, all based on SS-OCT. *Journal of Cataract and Refractive Surgery*, 49(1), 5–10. Available from: <https://doi.org/10.1097/j.jcrs.0000000000001023>
- Garza-Leon, M., Fuentes-de la Fuente, H.A. & García-Treviño, A.V. (2017) Repeatability of ocular biometry with IOLMaster 700 in subjects with clear lens. *International Ophthalmology*, 37(5), 1133–1138. Available from: <https://doi.org/10.1007/s10792-016-0380-7>

- Haigis, W., Lege, B., Miller, N. & Schneider, B. (2000) Comparison of immersion ultrasound biometry and partial coherence interferometry for intraocular lens calculation according to Haigis. *Graefes Archive for Clinical and Experimental Ophthalmology*, 238(9), 765–773. Available from: <https://doi.org/10.1007/s00417000188>
- Hirnschall, N., Findl, O., Bayer, N., Leissner, C., Norrby, S., Zimper, E. et al. (2020) Sources of error in toric intraocular lens power calculation. *Journal of Refractive Surgery*, 36(10), 646–652. Available from: <https://doi.org/10.3928/1081597X-20200729-03>
- Huang, J., Chen, H., Li, Y., Chen, Z., Gao, R., Yu, J. et al. (2019) Comprehensive comparison of axial length measurement with three swept-source OCT-based biometers and partial coherence interferometry. *Journal of Refractive Surgery*, 35(2), 115–120. Available from: <https://doi.org/10.3928/1081597X-20190109-01>
- Huang, J., Savini, G., Hoffer, K.J., Chen, H., Lu, W., Hu, Q. et al. (2017) Repeatability and interobserver reproducibility of a new optical biometer based on swept-source optical coherence tomography and comparison with IOLMaster. *The British Journal of Ophthalmology*, 101(4), 493–498. Available from: <https://doi.org/10.1136/bjophthalmol-2016-308352>
- Kunert, K.S., Peter, M., Blum, M., Haigis, W., Sekundo, W., Schütze, J. et al. (2016) Repeatability and agreement in optical biometry of a new swept-source optical coherence tomography-based biometer versus partial coherence interferometry and optical low-coherence reflectometry. *Journal of Cataract and Refractive Surgery*, 42(1), 76–83. Available from: <https://doi.org/10.1016/j.jcrs.2015.07.039>
- Langenbacher, A., Schrecker, J., Eppig, T., Schröder, S., Cayless, A., Schwemm, M. et al. (2022) Ratio of torus and equivalent power to refractive cylinder and spherical equivalent in phakic lenses – a Monte–Carlo simulation study. *Acta Ophthalmologica*, 100(1), 58–67. Available from: <https://doi.org/10.1111/aos.14902>
- Langenbacher, A., Szentmáry, N., Cayless, A., Weisensee, J., Fabian, E., Wendelstein, J. et al. (2021) Considerations on the Castrop formula for calculation of intraocular lens power. *PLoS One*, 16(6), e0252102. Available from: <https://doi.org/10.1371/journal.pone.0252102>
- Langenbacher, A., Szentmáry, N., Cayless, A., Weisensee, J., Wendelstein, J. & Hoffmann, P. (2021) The Castrop formula for calculation of toric intraocular lenses. *Graefes Archive for Clinical and Experimental Ophthalmology*, 259(11), 3321–3331. Available from: <https://doi.org/10.1007/s00417-021-05287-w>
- Liou, H.L. & Brennan, N.A. (1997) Anatomically accurate, finite model eye for optical modeling. *Journal of the Optical Society of America. A, Optics, Image Science, and Vision*, 14(8), 1684–1695. Available from: <https://doi.org/10.1364/josaa.14.001684>
- Lu, W., Li, Y., Savini, G., Song, B., Hu, Q., Wang, Q. et al. (2019) Comparison of anterior segment measurements obtained using a swept-source optical coherence tomography biometer and a Scheimpflug-Placido tomographer. *Journal of Cataract and Refractive Surgery*, 45(3), 298–304. Available from: <https://doi.org/10.1016/j.jcrs.2018.10.033>
- Lumme, S., Sund, R., Leyland, A.H. & Keskimäki, I. (2015) A Monte Carlo method to estimate the confidence intervals for the concentration index using aggregated population register data. *Health Services & Outcomes Research Methodology*, 15(2), 82–98. Available from: <https://doi.org/10.1007/s10742-015-0137-1>
- Martínez-Albert, N., Esteve-Taboada, J.J., Montés-Micó, R., Fernández-Vega-Cueto, L. & Ferrer-Blasco, T. (2019) Repeatability assessment of biometric measurements with different refractive states and age using a swept-source biometer. *Expert Review of Medical Devices*, 16(1), 63–69. Available from: <https://doi.org/10.1080/17434440.2019.1557517>
- Norrby, N.E., Grossman, L.W., Geraghty, E.P., Kreiner, C.F., Mihori, M., Patel, A.S. et al. (1996) Accuracy in determining intraocular lens dioptric power assessed by interlaboratory tests. *Journal of Cataract and Refractive Surgery*, 22(7), 983–993. Available from: [https://doi.org/10.1016/s0886-3350\(96\)80204-5](https://doi.org/10.1016/s0886-3350(96)80204-5)
- Norrby, S. (2008) Sources of error in intraocular lens power calculation. *Journal of Cataract and Refractive Surgery*, 34(3), 368–376. Available from: <https://doi.org/10.1016/j.jcrs.2007.10.031>
- Ophthalmic Implants – Intraocular Lenses. (2014) Part 2: Optical properties and test methods (ISO 11979-2:2014); EN ISO 11979-2.
- Panthier, C., Rouger, H., Gozlan, Y., Moran, S. & Gatinel, D. (2022) Comparative analysis of 2 biometers using swept-source OCT technology. *Journal of Cataract and Refractive Surgery*, 48(1), 26–31. Available from: <https://doi.org/10.1097/j.jcrs.00000000000000704>
- Preußner, P.R., Olsen, T., Hoffmann, P.C. & Findl, O. (2008) Intraocular lens calculation accuracy limits in normal eyes. *Journal of Cataract and Refractive Surgery*, 34(5), 802–808.
- Sabatino, F., Findl, O. & Maurino, V. (2016) Comparative analysis of optical biometers. *Journal of Cataract and Refractive Surgery*, 42(5), 685–693. Available from: <https://doi.org/10.1016/j.jcrs.2016.01.051>
- Sabatino, F., Matarazzo, F., Findl, O. & Maurino, V. (2019) Comparative analysis of 2 swept-source optical coherence tomography biometers. *Journal of Cataract and Refractive Surgery*, 45(8), 1124–1129. Available from: <https://doi.org/10.1016/j.jcrs.2019.03.020>
- Savini, G., Taroni, L., Schiano-Lomoriello, D. & Hoffer, K.J. (2021) Repeatability of total keratometry and standard keratometry by the IOLMaster 700 and comparison to total corneal astigmatism by Scheimpflug imaging. *Eye (London, England)*, 35(1), 307–315. Available from: <https://doi.org/10.1038/s41433-020-01245-8>
- Schiano-Lomoriello, D., Hoffer, K.J., Abicca, I. & Savini, G. (2021) Repeatability of automated measurements by a new anterior segment optical coherence tomographer and biometer and agreement with standard devices. *Scientific Reports*, 11(1), 983. Available from: <https://doi.org/10.1038/s41598-020-79674-4>
- Scholtz, S., Cayless, A. & Langenbacher, A. (2021) Calculating the human eye—basics on biometry. In: Liu, C. & Shalaby Bardan, A. (Eds.) *Cataract surgery*. Cham, Switzerland: Springer International Publishing AG. Available from: https://doi.org/10.1007/978-3-030-38234-6_7
- Shetty, N., Kaweri, L., Koshy, A., Shetty, R., Nuijts, R.M.M.A. & Sinha Roy, A. (2021) Repeatability of biometry measured by three devices and its impact on predicted intraocular lens power. *Journal of Cataract and Refractive Surgery*, 47(5), 585–592. Available from: <https://doi.org/10.1097/j.jcrs.0000000000000494>
- Wendelstein, J., Hoffmann, P., Hirnschall, N., Fischering, I.R., Mariacher, S., Wingert, T. et al. (2022) Project hyperopic power prediction: accuracy of 13 different concepts for intraocular lens calculation in short eyes. *The British Journal of Ophthalmology*, 106(6), 795–801. Available from: <https://doi.org/10.1136/bjophthalmol-2020-318272>
- Wylęgała, A., Bolek, B., Mazur, R. & Wylęgała, E. (2020) Repeatability, reproducibility, and comparison of ocular biometry using a new optical coherence tomography-based system and another device. *Scientific Reports*, 10(1), 14440. Available from: <https://doi.org/10.1038/s41598-020-71192-7>

How to cite this article: Langenbacher, A., Hoffmann, P., Cayless, A., Bolz, M., Wendelstein, J. & Szentmáry, N. (2024) Impact of uncertainties in biometric parameters on intraocular lens power formula predicted refraction using a Monte-Carlo simulation. *Acta Ophthalmologica*, 102, e285–e295. Available from: <https://doi.org/10.1111/aos.15726>